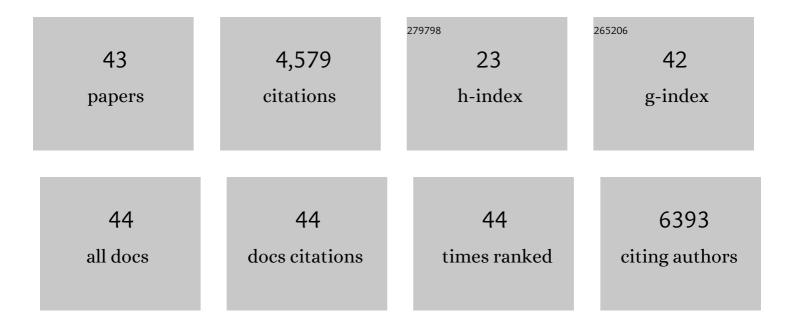
## Andreas M Loening

List of Publications by Year in descending order

Source: https://exaly.com/author-pdf/8768396/publications.pdf Version: 2024-02-01



#	Article	IF	CITATIONS
1	Diagnostic Performance of 9 Quantitative Ultrasound Parameters for Detection and Classification of Hepatic Steatosis in Nonalcoholic Fatty Liver Disease. Investigative Radiology, 2022, 57, 23-32.	6.2	15
2	Lymphatic regeneration after implantation of aligned nanofibrillar collagen scaffolds: Preliminary preclinical and clinical results. Journal of Surgical Oncology, 2022, 125, 113-122.	1.7	14
3	Renal Artery Variations in Patients With Mild-to-Moderate Hypertension From the RADIANCE-HTN SOLO Trial. Cardiovascular Revascularization Medicine, 2022, 39, 58-65.	0.8	3
4	Upstream Machine Learning in Radiology. Radiologic Clinics of North America, 2021, 59, 967-985.	1.8	9
5	Simultaneous PET/MRI in the Evaluation of Breast and Prostate Cancer Using Combined Na[18F] F and [18F]FDG: a Focus on Skeletal Lesions. Molecular Imaging and Biology, 2020, 22, 397-406.	2.6	14
6	How Often is the Dynamic Contrast Enhanced Score Needed in PI-RADS Version 2?. Current Problems in Diagnostic Radiology, 2020, 49, 173-176.	1.4	7
7	A New Multimodel Machine Learning Framework to Improve Hepatic Fibrosis Grading Using Ultrasound Elastography Systems from Different Vendors. Ultrasound in Medicine and Biology, 2020, 46, 26-33.	1.5	10
8	Variable Refocusing Flip Angle Single-Shot Imaging for Sedation-Free Fast Brain MRI. American Journal of Neuroradiology, 2020, 41, 1256-1262.	2.4	1
9	Conical ultrashort echo time (UTE) MRI in the evaluation of pediatric acute appendicitis. Abdominal Radiology, 2019, 44, 22-30.	2.1	4
10	The use of PET/MRI for imaging rectal cancer. Abdominal Radiology, 2019, 44, 3559-3568.	2.1	19
11	Viewâ€5haring Artifact Reduction With Retrospective Compressed Sensing Reconstruction in the Context of Contrastâ€Enhanced Liver MRI for Hepatocellular Carcinoma (HCC) Screening. Journal of Magnetic Resonance Imaging, 2019, 49, 984-993.	3.4	6
12	Prostate Magnetic Resonance Imaging Interpretation Varies Substantially Across Radiologists. European Urology Focus, 2019, 5, 592-599.	3.1	179
13	Structured Reporting of Multiphasic CT for Hepatocellular Carcinoma: Effect on Staging and Suitability for Transplant. American Journal of Roentgenology, 2018, 210, 766-774.	2.2	17
14	The impact of computed high b-value images on the diagnostic accuracy of DWI for prostate cancer: A receiver operating characteristics analysis. Scientific Reports, 2018, 8, 3409.	3.3	13
15	Prospective Evaluation of <sup>68</sup> Ga-RM2 PET/MRI in Patients with Biochemical Recurrence of Prostate Cancer and Negative Findings on Conventional Imaging. Journal of Nuclear Medicine, 2018, 59, 803-808.	5.0	70
16	Relative value of three whole-body MR approaches for PET-MR, including gadofosveset-enhanced MR, in comparison to PET-CT. Clinical Imaging, 2018, 48, 62-68.	1.5	1
17	Variable refocusing flip angle single-shot fast spin echo imaging of liver lesions: increased speed and lesion contrast. Abdominal Radiology, 2018, 43, 593-599.	2.1	2
18	Gallium 68 PSMA-11 PET/MR Imaging in Patients with Intermediate- or High-Risk Prostate Cancer. Radiology, 2018, 288, 495-505.	7.3	97

ANDREAS M LOENING

#	Article	IF	CITATIONS
19	Increased Speed and Image Quality for Pelvic Single-Shot Fast Spin-Echo Imaging with Variable Refocusing Flip Angles and Full-Fourier Acquisition. Radiology, 2017, 282, 561-568.	7.3	18
20	High temporal resolution dynamic MRI and arterial input function for assessment of GFR in pediatric subjects. Magnetic Resonance in Medicine, 2016, 75, 1301-1311.	3.0	7
21	Pilot Comparison of <sup>68</sup> Ga-RM2 PET and <sup>68</sup> Ga-PSMA-11 PET in Patients with Biochemically Recurrent Prostate Cancer. Journal of Nuclear Medicine, 2016, 57, 557-562.	5.0	155
22	<sup>68</sup> Ga-DOTA-Bombesin ( <sup>68</sup> Ga-RM2 or <sup>68</sup> Ga-Bombesin) PET versus <sup>68</sup> Ga-PSMA PET: A pilot prospective evaluation in patients with biochemical recurrence of prostate cancer Journal of Clinical Oncology, 2016, 34, 331-331.	1.6	2
23	Increased speed and image quality in singleâ€shot fast spin echo imaging via variable refocusing flip angles. Journal of Magnetic Resonance Imaging, 2015, 42, 1747-1758.	3.4	26
24	Faster pediatric 3-T abdominal magnetic resonance imaging: comparison between conventional and variable refocusing flip-angle single-shot fast spin-echo sequences. Pediatric Radiology, 2015, 45, 847-854.	2.0	8
25	Prospective Comparison of <sup>99m</sup> Tc-MDP Scintigraphy, Combined <sup>18</sup> F-NaF and <sup>18</sup> F-FDG PET/CT, and Whole-Body MRI in Patients with Breast and Prostate Cancer. Journal of Nuclear Medicine, 2015, 56, 1862-1868.	5.0	95
26	Engineering Luciferases for Assays and Imaging. , 2014, , 203-231.		2
27	A red-shifted Renilla luciferase for transient reporter-gene expression. Nature Methods, 2010, 7, 5-6.	19.0	144
28	Indirect imaging of cardiac-specific transgene expression using a bidirectional two-step transcriptional amplification strategy. Gene Therapy, 2010, 17, 827-838.	4.5	32
29	BRET3: a redâ€shifted bioluminescence resonance energy transfer (BRET)â€based integrated platform for imaging proteinâ€protein interactions from single live cells and living animals. FASEB Journal, 2009, 23, 2702-2709.	0.5	98
30	Cell-free metabolic engineering promotes high-level production of bioactive Gaussia princeps luciferase. Metabolic Engineering, 2008, 10, 187-200.	7.0	75
31	An Improved Bioluminescence Resonance Energy Transfer Strategy for Imaging Intracellular Events in Single Cells and Living Subjects. Cancer Research, 2007, 67, 7175-7183.	0.9	108
32	Crystal Structures of the Luciferase and Green Fluorescent Protein from Renilla reniformis. Journal of Molecular Biology, 2007, 374, 1017-1028.	4.2	130
33	Red-shifted Renilla reniformis luciferase variants for imaging in living subjects. Nature Methods, 2007, 4, 641-643.	19.0	277
34	Multimodality imaging of tumor xenografts and metastases in mice with combined small-animal PET, small-animal CT, and bioluminescence imaging. Journal of Nuclear Medicine, 2007, 48, 295-303.	5.0	116
35	Consensus guided mutagenesis of Renilla luciferase yields enhanced stability and light output. Protein Engineering, Design and Selection, 2006, 19, 391-400.	2.1	371
36	Self-illuminating quantum dot conjugates for in vivo imaging. Nature Biotechnology, 2006, 24, 339-343.	17.5	757

Andreas M Loening

#	Article	IF	CITATIONS
37	Creating self-illuminating quantum dot conjugates. Nature Protocols, 2006, 1, 1160-1164.	12.0	94
38	HaloTag Protein-Mediated Site-Specific Conjugation of Bioluminescent Proteins to Quantum Dots. Angewandte Chemie - International Edition, 2006, 45, 4936-4940.	13.8	153
39	Bifunctional antibody-Renilla luciferase fusion protein for in vivo optical detection of tumors. Protein Engineering, Design and Selection, 2006, 19, 453-460.	2.1	56
40	AMIDE: A Free Software Tool for Multimodality Medical Image Analysis. Molecular Imaging, 2003, 2, 131-137.	1.4	829
41	Whole-body skeletal imaging in mice utilizing microPET: optimization of reproducibility and applications in animal models of bone disease. European Journal of Nuclear Medicine and Molecular Imaging, 2002, 29, 1225-1236.	6.4	61
42	Injurious Mechanical Compression of Bovine Articular Cartilage Induces Chondrocyte Apoptosis. Archives of Biochemistry and Biophysics, 2000, 381, 205-212.	3.0	311
43	A versatile shear and compression apparatus for mechanical stimulation of tissue culture explants. Journal of Biomechanics, 2000, 33, 1523-1527.	2.1	162